**ASIAN JOURNAL OF CIVIL ENGINEERING (BHRC) VOL. 17, NO. 2 (2016)**
**PAGES 169-192**

# SIZE EFFECT SIMULATION OF SHEAR CRITICAL RC MEMBERS: LOCAL-AVERAGE STRESS FIELD APPROACH

A. Jahanmohammadi and M. Soltani*
Faculty of Civil and Environmental Engineering, Tarbiat Modares University, Jalaale-al Ahmad Ave, Tehran, Iran

**Received:** 10 May 2015; **Accepted:** 22 August 2015

## ABSTRACT

Accurate evaluation of RC members under shear is achieved by consideration of both size-dependency and participating local mechanisms. Following the fundamental concept of the smeared crack approach, local-average stress field concept is presented considering the localized and size-dependent characteristics. Adopting a proposed slip-strain model, application of local strain/stress information in combination with the average response is available. Accordingly, effective size-dependent parameters are included in the evaluation process; and the average and discrete responses are computationally updated regardless of the size-dependency limitations. The abilities of the proposed concept are discussed for size-dependent parameters and validated for shear-critical members.

**Keywords:** Smeared crack; local-average stress field; slip-strain relation; size effect; nonlinear finite element; shear-critical RC members.

## 1. INTRODUCTION

Detecting the shear failure in reinforced concrete members is an important topic in structural engineering researches. This is due to the sudden occurrence of the shear failure and involvement of several mechanisms in its formation. According to the extensive experimental and numerical researches, the behaviour of RC beams under shear, especially those with no transverse reinforcement, is known as a size-dependent response. In such beams, the nominal shear strength of the beam is gradually reduced as the beam depth increases. This is called the size effect on shear strength of RC members [1-2] and is studied through experimental, numerical and analytical investigations. In the outstanding experimental researches on this topic, the role of the effective depth in determining the shear strength of the beams with no shear reinforcement was investigated by Kani [3] and Iguro [4]. As a result, dependency of the shear response on the effective depth has been stated

*E-mail address of the corresponding author: msoltani@modares.ac.ir (M. Soltani)

even in deep specimens. Taylor [1] found that if the maximum aggregate size is in proportion to the depth, dependency of the shear response on the effective depth would be reduced. Following this idea, an experimental research was conducted by Shioya [5] in which, the aggregate size and flexural tensile strength of concrete were reported as the main factors causing the size effect. In addition, extensive testing programs conducted by Scordelis [6], Vecchio [7] and Collins [8], confirmed the size-dependent behavior of shear-critical beams even the ones with shear reinforcements. This means that the shear response could be related to both the size and the shear transfer mechanism along the crack plane. However, the shear transfer mechanism is inherently a size-dependent phenomenon.

Mentioned researches, and many other tests, were used to generate the design standards and to present the numerical relations for predicting the shear strength of RC members. In addition, analytical evaluation methods are developed in order to investigate the step-by-step response of RC members. The well-known smeared crack approach is one of the most powerful numerical methods for nonlinear analysis of RC members. This approach, which was extended by Maekawa [9], Vecchio and Collins [10-11], and Hsu [12-13], expresses the behavior of participating materials and their interaction by an average interpretation. In this regard, post-crack tensile behavior of steel and concrete are defined by average models [9-13]. Extensive experimental investigations, adopted for presenting the average concept of smeared crack approach, state the high dependency of the average models on the dimensional and behavioral characteristics participated in the post-crack response [9]. Initiating a crack, there is a zone which is affected by the occurred discontinuity in the continuum RC domain. Dimension of this zone can be regarded by the crack spacing, in the length, and crack depth, in the height. On the other side, extent of the mentioned length and height depends on the properties of concrete and steel bars and reinforcement arrangement. Size of aggregate, initial fracture energy of concrete, reinforcement diameter and the cover amount provided for steel bars are from the important characteristics contributing in the determination of the zone affected by the presence of a crack. Regarding the dimension of the detected zone, these characteristics are regarded in the definition of the average models of smeared crack approaches. However, some of them are known as the main causes of the localized mechanisms. Incidence of slip between the steel bar and its surrounded concrete, activating the bond-transfer mechanism, degradation in the shear strength due to the large crack opening and sliding are from the local mechanisms mainly induced by the mentioned characteristics. These mechanisms can be regarded individually as a discrete mechanism or can be extended trough the zone affected by the crack. Following each of these approaches decrees the use of additional theories which are in a reliable consistency with the basic concept of the smeared crack approach. Considering the numerical efforts and stability of the analysis, use of discrete approaches [14] is not recommended.

The most compatible concept following the fundamental theories of smeared crack approach has been presented by An [1-2], known as "*the zoning concept*". In this concept, the zone affected by the bond transfer mechanism is introduced as RC zone and the remaining part, as PL (plain) zone (Fig. 1). These zones are known as the control volume which is affected by the presence of cracks and steel bars. Adopting this concept, the control volume for determining the participation of each material, steel and concrete, is determined at the beginning of the analytical procedure.

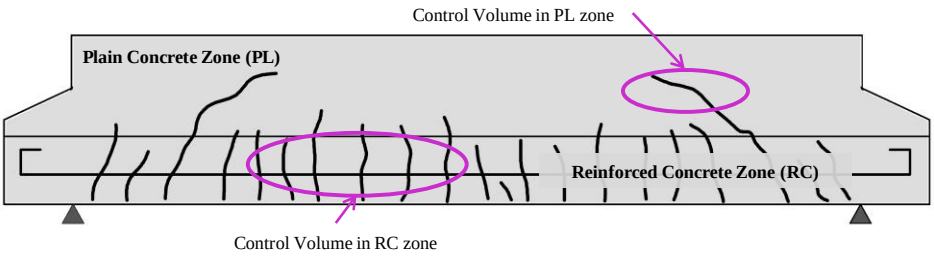


Figure 1. Definition of the zoning concept [1]

Although the mechanical properties of the materials and dimensional properties of the member are regarded in this concept, growth of the cracks is not considered trough the modeling procedure. This may not affect the accuracy of the zoning concept in evaluation of adequately reinforced members; however, it brings significant infirmities in numerical modeling of the lightly reinforced members or the members with high dependency to the previously mentioned mechanisms. It is remarkable that the lightly reinforced members experience only a few cracks in different loading steps with quite differences in corresponding displacements. This may result in step-by-step changes in the control volume and, consequently, the average behaviors of the material. Therefore, definition of the PL and RC zones regardless of the cracking procedure is not reliable in such members. In addition to the accurate estimation of the average models, precise modeling of the shear transfer mechanism in PL zone is of high importance, especially in shear-critical members. This mechanism, with a displacement-based formulation, must be updated for step-by-step changes in the values of opening and sliding at the crack plane.

Effective parameters in determining the reliable control volume of the smeared models are investigated in this paper. These parameters and the localized mechanisms induced by them are considered in a proposed "*Local-average stress field concept*". A nonlinear finite element program, ESMARC, is developed to consider the average-stress field concept of the smeared crack modeling and the local-stress field for evaluating the discussed parameters. It is enhanced with a proposed slip-strain model to express a reliable estimation of local information (strain and stress) where consequently conceives the application of the displacement-based shear models. The mentioned local-average stress field approach is discussed for the mentioned effective parameters, induced mechanisms, and their dependency to the size, and is validated by numerical assessment of shear-critical RC members. Regarding the results, the proposed approach is able to detect the zones affected by interaction of concrete and reinforcing bar; and to enhance the average responses in an updated control volume.

## 2. LOCAL-AVERAGE STRESS FIELD: CONCEPT

Formation of a crack is followed by occurrence of local displacement at the crack plane. This initiates the slip between concrete and steel bar and consequently activates the bond transfer mechanism. On the other side, sliding and opening of the crack plane motivates the shear transfer mechanism along the crack surface. The two mentioned mechanisms are inherently related to the mechanical and dimensional properties of material. Aggregate size

and fracture energy of concrete, diameter and arrangement of reinforcements, and the mechanical properties of both steel and concrete are from the effective parameters which must be regarded in accurate estimation of the post-crack behavior of RC members, especially lightly reinforce ones. Since the fundamental assumptions of the zoning concept [1] is not accurately validated for lightly reinforced member, the "Local-average stress field" concept is proposed in this research.

The concept considers the discrete discontinuities -specifically crack- by their exact responses; and evaluates the behavior of the zones in the vicinity of the crack -introduced by "*control volume*"- by their average responses. Considering the localized displacements at the crack surface, mechanisms mentioned in Fig. 2 are activated in the post-crack responses. These mechanisms are corresponded to the local behavior resulted at the crack interface, local contribution of concrete and steel bars at the crack plane, and average behavior of concrete and steel bars. Local behavior of the crack is determined by the localized shear transfer mechanism at the crack plane and is introduced by two stress components, "*Aggregate Interlock*" and "*Dilatancy*" (Fig. 2b). Amount of these components are directly related to the aggregate size and the amount of opening and sliding of the crack; all known as size-dependent parameters. On the other side, the stress component due to the local behavior of concrete at the crack surface is an interpretation for the release rate of tensile stress, *tension softening*. This size-dependent stress component (Fig. 2b) is known as the "*Bridging Stress*" and is fundamentally defined by the initial characteristics of concrete, as tensile strength, $f_{cr}$, fracture energy, $G_f$, and also the crack opening [9]. In addition, presence of steel bars in the crack plane is defined by two local stress components, normal and parallel to the crack plane (Fig. 2c). These components -in combination with the local stress components of shear and bridging at the crack plane- are interpreted by *tension stiffening* and *shear stiffening*, respectively (Fig. 2d). Contribution of reinforcing bars in the crack response may be considered independent of size, however, values of the participating stress components are determined based on local strain and stress of steel at the crack surface.

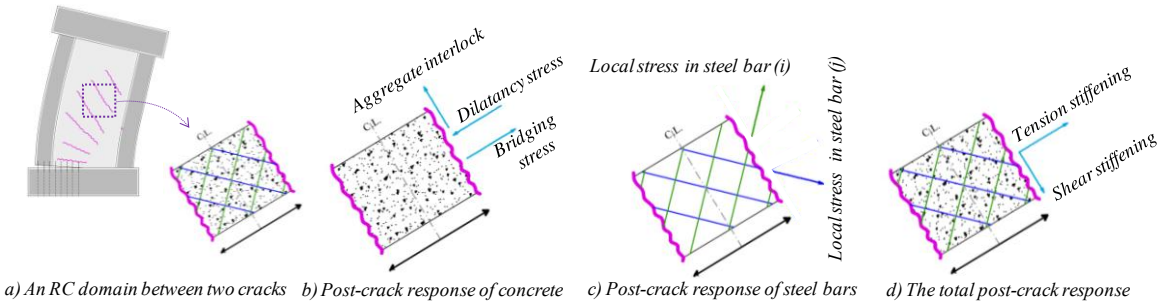


Figure 2. Localized post-crack mechanisms

In addition to the mentioned local components, amount of slip induced by the local displacements of the crack plane, will affect the distribution of the local strain along the steel bars. This may result in changing the distribution of the local strain and stress in the control volume; and consequently, the average behavior of materials in this domain. To bring the mentioned local mechanisms and their dependency to the size into the average response of RC members, "*local-average stress field*" concept is proposed in a step-by-step algorithm. This concept starts by detecting the cracked RC domain and ends having a relatively

accurate estimation on local characteristics. Adopting this concept in combination with the smeared crack approach, a nonlinear finite element program is developed. The program - known as ESMARC: *Enhanced Smeared Crack Analysis of RC members*- follows the nonlinear finite element analytical procedure specialized with the rules of smeared crack approach (Fig. 3). However, it is enhanced by a "*post-process*" procedure that is called at the end of a converged load step to bring the local strain/stress information into account.

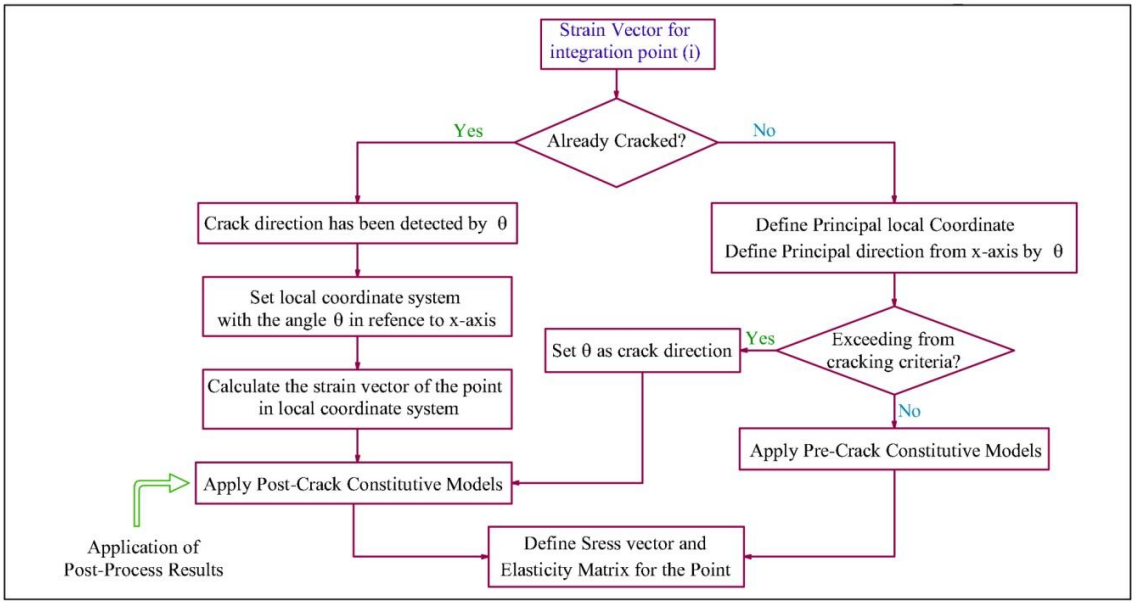


Figure 3. Summarized flowchart for nonlinear analysis of an RC integration point

Applying the proposed concept, average characteristics of smeared constitutive models of concrete and steel are updated, considering the participating local mechanisms including effective size-dependent factors. Main computational steps of the local-average stress field concept is introduced in Figs. 4 and 5, and is described as below:

*Step 1*- With the available information from the previous load step, the crack direction is known for a cracked integration point. Regarding the geometry of the problem, including dimensions and constraints, a "*control volume*" is determined. This domain hypothetically is limited between two parallel cracks; therefore, its length is introduced by the *crack spacing*.

*Step 2*- Knowing the average strain state in the control volume, the values of the crack opening ($\omega$) and sliding ($\delta$) are determined by Eq. 1 and Eq. 2. Values of the $\varepsilon_1$ and $\delta_{12}$ are related to the average tensile and shear strains and the values of $\varepsilon_{1cr}$ and $\delta_{12cr}$ are tensile and shear strains at the cracking state. Accordingly, the bridging stress ($\sigma_{brg}$) at the crack plane is defined by Eq. 3.

$$\omega = (\varepsilon_1 - \varepsilon_{1cr}) \times Crack\ Spacing \tag{1}$$

$$\delta = (\gamma_{12} - \gamma_{12cr}) \times Crack\ Spacing \tag{2}$$

$$\sigma_{brg} = f_{cr}\left(1 + 0.5\omega\left(\frac{f_{cr}}{G_f}\right)\right)^{-3.0} \tag{3}$$

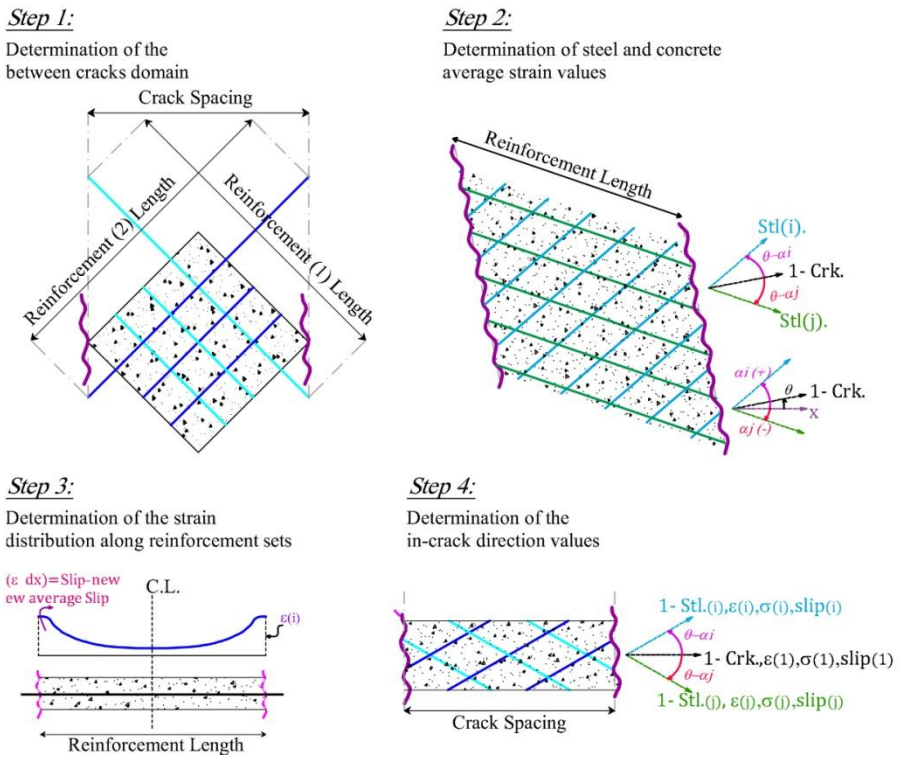


Figure 4. Main steps of Local-Average stress field concept

Similarly, by detecting the average tensile strain of each steel set, slip value of each set at the crack surface is also calculated by multiplying the corresponding average tensile strain in corresponding reference length. The reference length is known as the length in which the bond stress must be transferred. In some cases, especially in direct tension case where the crack spacing is small, the reference length will be half of the embedment length of the bar. This length is determined in reference to the crack spacing and the steel bar direction by Eq. 4. In which $\theta$ is the angle between the global $x$-axis and direction 1 of the crack, and $\alpha$ is the angle between the global $x$-axis and rebar direction. However, in the cases with large crack spacing, the bond stress is transferred in a specific part of the embedded length, so the reference length will be equal to the bond transfer length.

$$L_{steel} = \frac{Crack\ Spacing}{\cos(\theta - \alpha)} \tag{4}$$

*Step 3*- Local strain profile for each reinforcement set, embedded in this domain, is estimated by use of the proposed slip-strain relation. Consequently, the local stress will be defined with the aid of the bare bar strain-stress model [9].

*Step 4*- Concentrating on control volume in the direction orthogonal to the crack plane, each steel sets' information will be transferred in this direction. Therefore, local and average resultant stress components of both steel and concrete on the crack surface are evaluated. Having the resultant stress components normal to the crack surface, two "*tensile stress equilibrium conditions*" will be checked in steps 5 and 6. The first; locally controls the new crack development, and the second; determines the new average properties of the steel bar and concrete.

*Step 5*- New crack initiation is probable if the maximum concrete stress at the centerline of the crack spacing ($\sigma_{max.con}$) exceeds the tensile strength of concrete. This stress is the only unknown value in the local equilibrium condition and must be in equilibrium with already known values of maximum steel stress ($\sigma_{max.steel}$) and bridging stress ($\sigma_{brg}$) at the crack plane and minimum steel stress at the centerline ($\sigma_{min.steel}$), Fig. 5a. It is remarkable that with each new crack development, steps 2 to 4 will be repeated till there would be no hope for new crack happening.

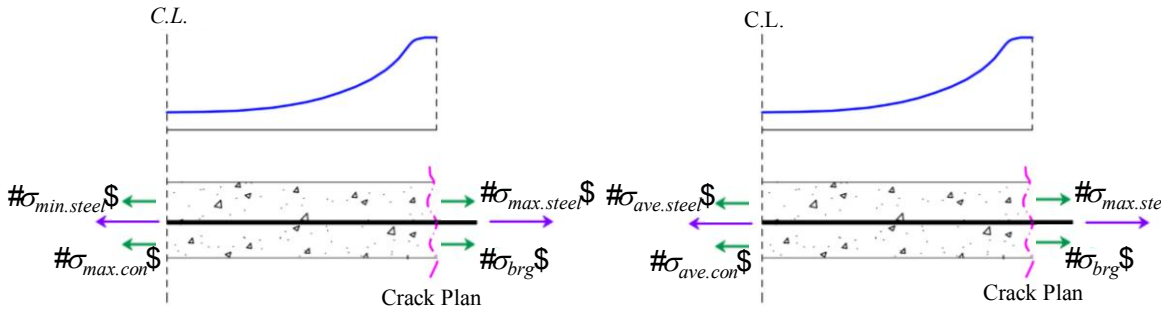


a) Local stress equilibrium condition b) Local-average stress equilibrium condition

Figure 5. Stress equilibrium condition of Local-Average stress field concept

*Step 6*- Stabilizing the crack spacing, average response of concrete and steel are re-evaluated. Based on average tensile stress equilibrium condition, the average stress for concrete at the centerline of the crack spacing ($\sigma_{ave.con}$) is the unknown value while maximum steel stress ($\sigma_{max.steel}$) and bridging stress ($\sigma_{brg}$) at the crack plane and average stress of steel ($\sigma_{ave.steel}$) at the centerline are known (Fig. 5b). Satisfying this equilibrium condition, modifications on average characteristics of concrete and steel bars -the release in post-cracking tensile stress of concrete and decrease in the average yield strength of each reinforcing set- are evaluated. Computational details of these modifications are presented in section 3.

*Step 7*- Determining the new values for average characteristics, updated average models for concrete and steel will be introduced for the behavior of RC integration points in the control volume.

## 3. LOCAL-AVERAGE STRESS FIELD: SIZE-EFFECT INCLUDED COMPUTATIONAL DETAILS

Proposed local-average stress field approach is conceptually applicable in combination with

all available smeared crack approaches. In order to consider the exact modelling of local shear transfer mechanism along the crack plane, the fixed-smeared crack approach is followed in this research. In addition, the average constitutive models presented by Maekawa et al [9], have specific definitions for the average characteristics, as for tension softening of concrete and average yield strength for steel. To discuss the outstanding features of the proposed approach, these models are adopted in computational procedure of the mentioned local-average stress field concept. In this regard, detecting the bond- and crack-influencing zone is firstly investigated for accurate estimation of the reference control volume. After that, the slip-strain model which is used to represent the local strain distribution along the embedded reinforcing bar is presented with all included parameters, especially size-dependent ones. Updating the constitutive models of concrete and steel, in reference to both local mechanisms and size-dependent parameters is discussed at the end of this section. Having the computational details discussed herein, the step-by-step algorithm introduced in previous section will result in accurate and enhanced estimation of local, average and overall response of RC members.

*3.1 Reference control volume*

Local displacements, induced by formation of a crack, spread through the zone which is affected by the local characteristics of the crack. The extent of this zone, known as the control volume, is directly affected by presence and arrangements of reinforcing bars. However, un-reinforced zones can be defined regarding the local characteristics of concrete. To introduce a reliable estimation of the length and width of the control volume into the numerical analysis, a local detecting procedure must be conducted, considering the step-by-step updates during the analytical process.

To enhance the local-average stress field concept, a proposed strain-evaluating approach is applied into the developed program of ESMARC. In this regard, the geometry of the RC member is considered with all of its integration points. At the beginning of the analysis, the overall geometry is inspected for classifying the integration points with same horizontal / vertical coordinates. Accordingly, a set of points are detected for horizontal and vertical neighbourhood of each integration point. In each loading step, calculated strain of each integration point is controlled to detect the changes in dimension of the cracked zone. Describing the procedure for point (i), four main directions of Left, Right, Bottom and Top are considered for the point. If (i) is reported as a cracked point, its neighbour points are checked for cracking state toward mentioned directions, individually (Fig. 6a). For each direction, the extent length of the cracked zone is determined by the distance of the point (i) from the point (j), where point (j) is the last cracked point in neighbourhood (Fig. 6b). Having the left and right lengths, the reference length of the control volume is detected; in addition, sum of the top and bottom lengths will result in determination of the reference height.

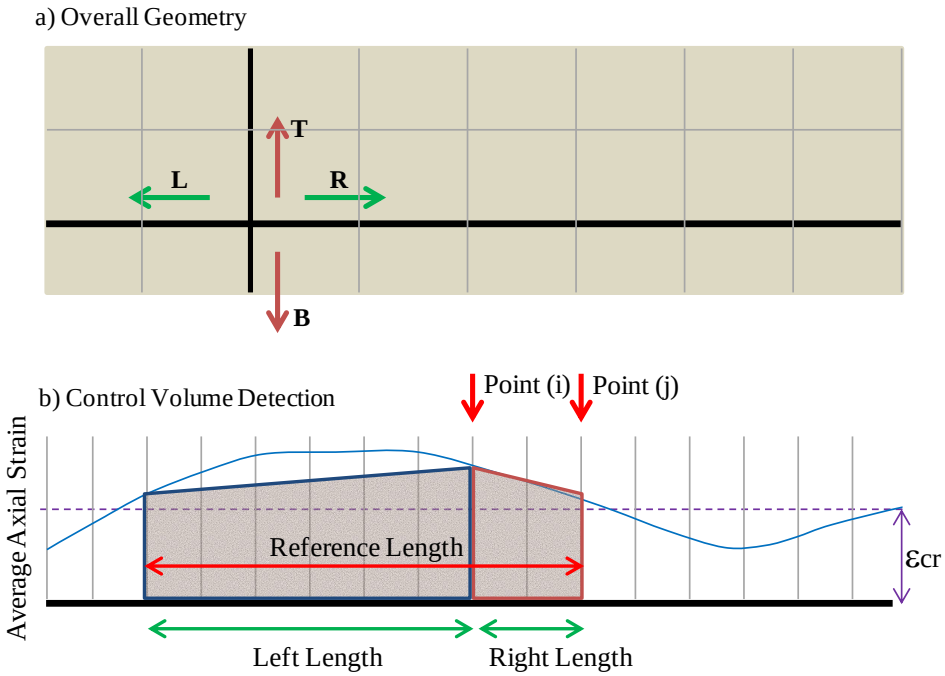


Figure 6. Strain-evaluating approach for detecting the control volume

By determining the dimensions of the control volume, local-average stress field computations are applied and the probable cracks in this domain are detected (step 5). It is noteworthy that the control volume is gradually extended by the crack progression. However, presence of a crack and the amount of the transferred bond stress between steel bar and its surrounded concrete can eliminate the effective dimension of the control volume. This is considered by the definition of bond- and crack-influencing zones where the first, defines the limit height and the second, defines the limit length of the control volume.

Presence and arrangements of reinforcing bars, even horizontal and transverse, defines the bond-influencing zone. Length of this zone can be regarded as the crack spacing, and height of it can be interpreted by the depth of a crack, because the bond stress is vertically vanished at the crack tips. These limitations are applied to define the reference length and height. However, continuance of the analytical procedure will change the way of occurrence of the cracks. First developed cracks are the ones which are initiated from the cover. These cracks are known as primary cracks and spread in approximately whole tensile height of the cross section. Stabilizing the primary cracks, the secondary cracks are developed. These cracks are initiated from the reinforcing bar elevation. As discussed by Broms et al. [15], height of these cracks are limited up to the twice of the developed cover for each reinforcing bar, or the distance between two adjacent reinforcing bars. On the other side, minimum spacing of secondary cracks is introduced by quarter of the latest value reported for the primary crack spacing [15]. Therefore, conducting the local-average stress field computational procedure must be followed by controlling the minimum values for dimensions of the control volume by applying the discussed limitations. This is adopted in the developed program of ESMARC and as a consequence, dependency of the size is automatically introduced into the nonlinear analysis of RC members.

*3.2 Local strain distribution*

Following the idea presented by Shima [16], Shin [9], Soltani [17], and considering the complete modeling of steel-concrete interaction as in universal bond-slip-strain model of Shima [16], a unified slip-strain model is proposed to adopt in local-average stress field concept. The model describes the local strain distribution along the embedded steel bars surrounded by concrete. Evaluation of the steel bar's behavior in the axial tension case with any embedment length is applicable with the proposed model. The model is also valid for assessing the behavior of steel bar in the pull out case with an adequate embedment length. It is also enriched by introducing the effects of the developed cover, presence and amount of stirrups and bond deterioration zone which are known as size-dependent parameters [18-19].

The proposed model expresses the explicit relation between non-dimensional slip value and local strain for a wide range of strains, including pre- and post-yield behavior. Changes of the slip-strain relation in different strain ranges are defined by Eq. 5.

$$\begin{aligned} s &= \varepsilon_s\left(a + 3500\varepsilon_s\right) && \varepsilon \le \varepsilon_y \\ s_y &= \varepsilon_y\left(a + 3500\varepsilon_y\right) \\ s &= s_y + \frac{0.04 s_y}{\left(\varepsilon_{sh} - \varepsilon_y\right)}\left(\varepsilon_s - \varepsilon_y\right) && \varepsilon_y \le \varepsilon \le \varepsilon_{sh} \\ s &= 1.04 s_y + 0.1\left(f_u - f_y\right)\left(\varepsilon_s - \varepsilon_{sh}\right) && \varepsilon \ge \varepsilon_{sh} \end{aligned} \tag{5}$$

where $s$ is the non-dimensional slip, $\varepsilon_s$ is the local strain on steel bar, $\varepsilon_y, \varepsilon_{sh}, f_u, f_y$ are the behavioral characteristics of steel, $s_y$ is the non-dimensional yield slip and $a$ is the degradation parameter defines the reduction in the local strain distribution. Non-dimensional slip value of $s$ is related to the dimensional slip value of each reinforcing set. This slip which is introduced by $S$ is commonly calculated multiplying the average tensile strain by corresponding reference length. However, dependency of size and the inclination of each reinforcing bar from the crack plane are from the important parameters which must be considered in determination of this slip value. In this regard, values of opening and sliding on the crack surface are determined by Eqs. 1 and 2. Contribution of these two displacements in determining the accurate value of slip is defined by Eq. 6 [9].

$$S = [\delta \cos(\theta - \alpha) + \omega \sin(\theta - \alpha)] \tag{6}$$

Equations 7 through 10 explain the normalization of the dimensional slip value to the non-dimensional one. In these equations, $d$ and $f'_c$ are the rebar diameter and concrete compressive strength; $K_{fc}$ is a coefficient describing the effect of concrete's compressive strength (Eq. 8); $C_5$ is introduced considering the amount of the clear cover (Eq. 9) and $\Omega$ is the stirrup index of confinement which is determined as an equivalent cover coefficient considering the presence of stirrups (Eq. 10). This index is determined regarding Fig. 7 in which $A_{st}$ is the total area of the legs of stirrup, $S_{st}$ is the spacing of the stirrups, and $n$ is the number of the longitudinal reinforcing bars confined by the stirrup.

$$s = \frac{S}{d} K_{f_c} C_5 \tag{7}$$

$$K_{f_c} = \left(f'_c / 20\right)^{2/3} \tag{8}$$

$$C_5 = \left( \frac{\left( \frac{\text{cov er}}{d} + 33\Omega \right)}{3} \right)^{2/3} \leq 1.2 \tag{9}$$

$$\Omega = \frac{A_{st}}{n.S_{st}.d} \tag{10}$$

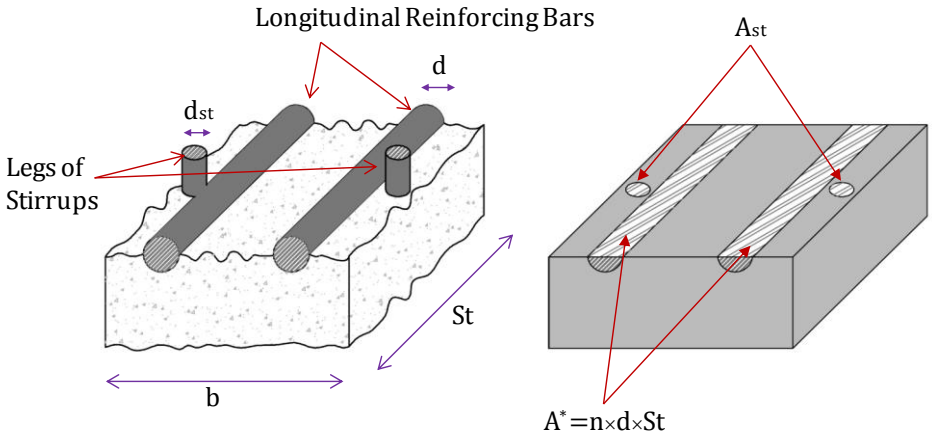


Figure 7. General parameters of the stirrup index of confinement [19]

Following the equations of 5~10, the local post-crack response of a reinforcing bar embedded in an RC domain is evaluated considering the rebar diameter, cover and stirrups. Dependency of this response to one of the most important size-dependent parameters –crack spacing- is also introduced in the model. This is defined by considering the distance of any distinct point on the rebar from the crack plane. For this aim, four main zones are determined in the local strain distribution (Fig. 8). These zones are defined form the crack surface toward the fixed boundary as: 1) the bond deterioration zone (*A*~*C*), 2) the zone with the sharp-decrease in local strain (*C*~*D*), 3) the zone with the soft-decrease in local strain (*D*~*E*) and 4) the zone affected by the fixed end properties (*E*~*F*). Effect of the distance from the crack in slip-strain response of each point -located in first three zones- is determined by a variable degradation parameter of '*a*'. This parameter smoothly varies from the crack interface toward the fixed end by Eq. 11. The fourth zone is defined to overcome the uncertainty of the local strain distribution in the locations near the fixed end of a not-adequately embedded bar. This zone is introduced with the length of $0.125(L\text{-}L_b)$ and its local strain is constantly set equal to the strain value in point *E*.

$$\begin{aligned} a &= 6.0 - 3.0\left(\frac{x}{L_b}\right) && x \le L_b \\ a &= 3.0 && L_b \le x \le 0.5(L + L_b) \\ a &= 3.0 - 3.0\left(\frac{x - 0.5(L + L_b)}{0.5(L - L_b)}\right) \ge 0.1 && x \ge 0.5(L + L_b) \end{aligned} \tag{11}$$

Here, "*L*" is defined as the reference length; "*x*" is the location of a point on the rebar, which is set to zero at the free end of rebar. $L_b$ is the bond deterioration zone – simultaneously related to the rebar diameter and the clear cover- and is introduced by Eq. 12.

$$\begin{aligned} L_b &= 5.0d/(Cover/5d)^{2/3} && if\ L \ge 10.0d/(Cover/5d)^{2/3} \\ L_b &= L - 5.0d/(Cover/5d)^{2/3} && if\ 5.0d/(Cover/5d)^{2/3} \le L \le 10.0d/(Cover/5d)^{2/3} \\ L_b &= 0.0 && if\ L < 5.0d/(Cover/5d)^{2/3} \end{aligned} \tag{12}$$

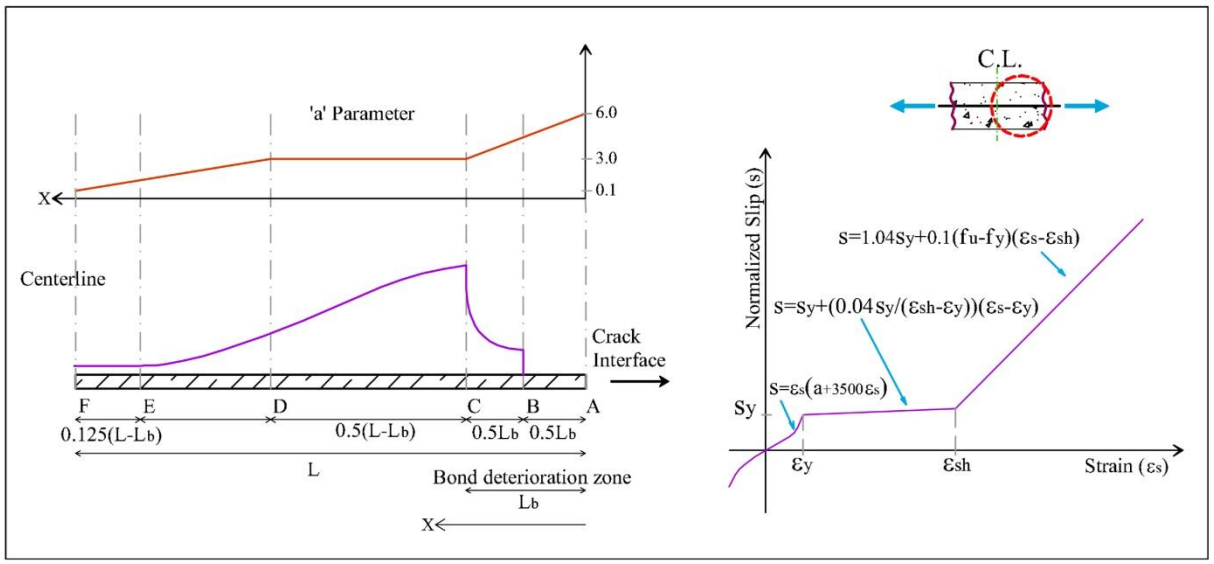


Figure 8. Proposed slip-strain model

*3.3 Updated constitutive models*

As mentioned before, the constitutive models presented by researchers of University of Tokyo [9] are applied in current manuscript. These models are divided into pre- and post-crack phase models as presented in Fig. 9. The models of average tensile behavior of concrete, average tensile behavior of steel and the shear transfer mechanism are dependent on both the size of the control volume and the local properties of the cracking states. Whereas, the bare bar model of steel [20] and the uni-axial and biaxial compression models of concrete [9, 21] are defined regardless of the zoning concept. Therefore, the first set of the models are discussed in this part and the readers are requested to review the second set in corresponding references.

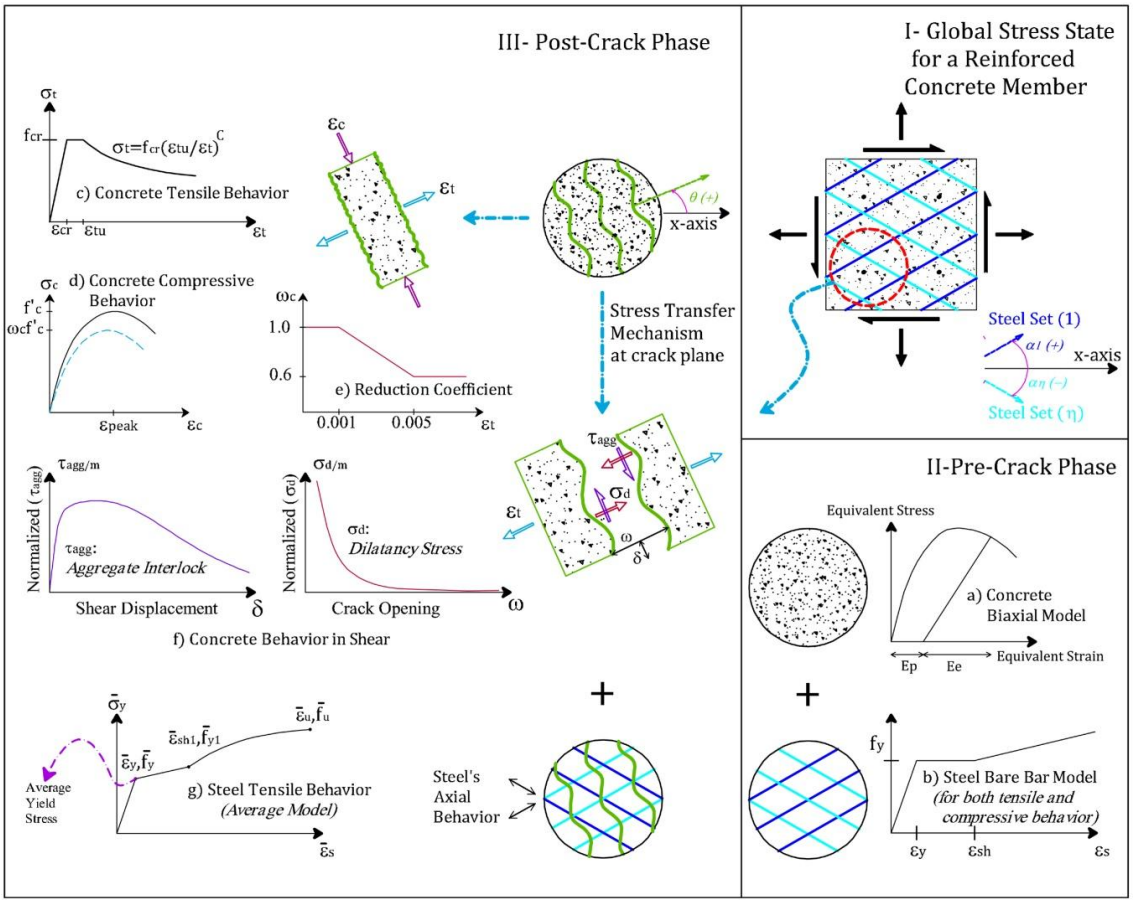


Figure 9. Schematic introduction of the constitutive models adopted in ESMARC

*3.3.1 Average tensile behavior of concrete*

Tensile behavior of concrete is computationally modelled by a linear pre-crack response and a nonlinear post-crack behavior (Eq. 13). The post-crack response is formulated by a release in the tensile behavior which is expressed in terms of cracking strain and strength, $\varepsilon_{cr}$, $f_{cr}$, tension softening/stiffening parameter, $C$, and average tensile strain, $\varepsilon$. The zoning concept of An [1] reports a size-dependent value of $C$ for the un-reinforced concrete and a predefined value for reinforced concrete. Whereas, the proposed local-average stress field concept enriches the zoning concept with local-average-based update of the $C$ parameter. Regarding the local and average stress state discussed in step 6 of the computational procedure, values of the average tensile strain and stress at current loading state ($\varepsilon_{ave.con}$, $\sigma_{ave.con}$) are known. Accordingly, by using the post-crack relation of Eq. 13, value of tension softening/stiffening parameter is determined for each loading state (Fig 10.a). It is remarkable that this procedure is independent of the predefined judgment about the presence of reinforcing bars and amount of them.

$$\begin{array}{lll} \sigma = E_c \varepsilon & \varepsilon \le \varepsilon_{cr} & \varepsilon_{tu} = 2\varepsilon_{cr} \\ \sigma = f_{cr} & \varepsilon_{cr} \le \varepsilon \le \varepsilon_{tu} \quad \textit{in which:} & f_{cr} = 0.33\sqrt{f_c'} \quad (MPa) \\ \sigma = f_{cr}\left(\dfrac{\varepsilon_{tu}}{\varepsilon}\right)^c & \varepsilon \ge \varepsilon_{tu} & E_c = 5000\sqrt{f_c'} \quad (MPa) \end{array} \tag{13}$$

*3.3.2 Average tensile behavior of steel*

Average tensile behavior of steel is expressed by average tri-curved model, represented by Maekawa and Salem [22]. In this model, Eq. 14, $\bar{\varepsilon}_y$ is the average yield strain, $\bar{f}_y$ is the average yield stress; $\bar{\varepsilon}$ and $\bar{\sigma}$ are average strain and stress, respectively, and $E_s$ is elasticity modulus of steel. $\bar{\varepsilon}_y$ and $\bar{f}_y$ are the average characteristics of steel and are determined in the post-processing procedure regarding the localized effects. The points with average strain-stress coordinates of ($\bar{\varepsilon}_y$ - $\bar{f}_y$) and ($\bar{\varepsilon}_{sh1}$ - $\bar{f}_{y1}$) are used to express average yield and hardening states, respectively. Average ultimate stress for steel is also defined by $\bar{f}_u$ and $k$ is $0.035(400/f_y)^{1/3}$ in (MPa).

$$\begin{array}{ll} \bar{\sigma} = E_s \bar{\varepsilon} & \bar{\varepsilon} \le \bar{\varepsilon}_y \\ \bar{\sigma} = \bar{f}_y + \left(\dfrac{\bar{\varepsilon} - \bar{\varepsilon}_y}{\bar{\varepsilon}_{sh1} - \bar{\varepsilon}_y}\right)\left(\bar{f}_{y1} - \bar{f}_y\right) & \bar{\varepsilon}_y \le \bar{\varepsilon} \le \bar{\varepsilon}_{sh1} \\ \bar{\sigma} = \bar{f}_{y1} + \left(1 - \exp\left(\dfrac{\bar{\varepsilon}_{sh1} - \bar{\varepsilon}}{k}\right)\right)\left(1.01\,\bar{f}_u - \bar{f}_{y1}\right) & \bar{\varepsilon} \ge \bar{\varepsilon}_{sh1} \end{array} \tag{14}$$

Average yield strength, $\bar{f}_y$, as the main average characteristics of the steel model [9,22], is introduced with respect to the zoning effect. Value of the average yield stress is commonly less than the reported yield strength of a bare bar (Fig. 10b) and is evaluated for each reinforcing set regarding the reinforcement ratio, properties of the surrounded concrete, and the bond transfer mechanism. In current study, the average yield stress of reinforcing bar is associated with the case in which only one point on the embedded bar – specifically the point in the crack location- exceeds the yield strain, $\varepsilon_y$. To simulate this case, the approach discussed in step 2 of the local-average stress field procedure is adopted. For this aim, the initial value of slip for each reinforcing bar is set equal to the bar's yield slip ($crack\ spacing \times \varepsilon_y$). Having the local strain distribution of the yield state, the local stress distribution is known by applying the bare bar model of steel [9]. Values of the average yield strain and stress for reinforcing bar is calculated by integrating the area under the local profile of strain and stress, respectively (Fig. 10c).

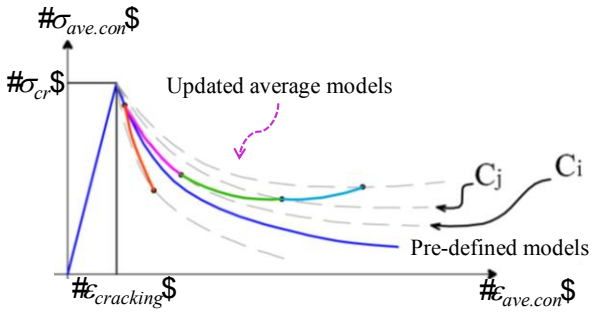


a) Updated average model for concrete

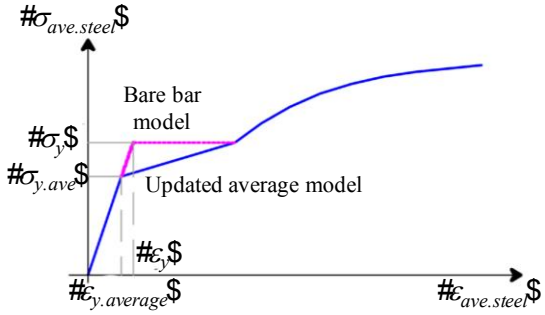


b) Strain/stress distribution at the yield point

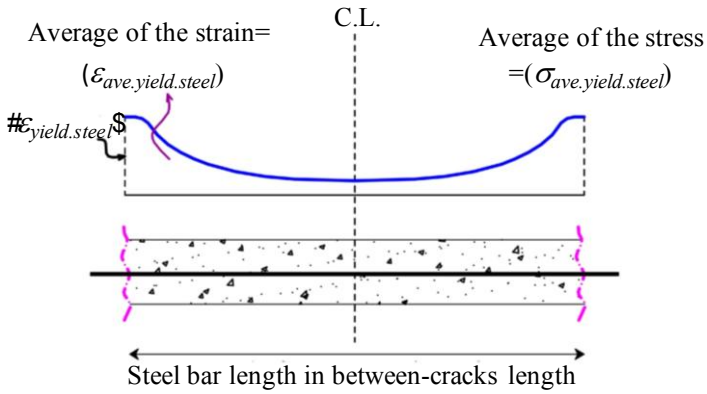


c) Strain/stress distribution at the yield point

Figure 10. Average constitutive models updated by local information

*3.3.3 Shear transfer mechanism*

The shear transfer mechanism is commonly introduced by two main stress components including the dilatancy stress ($\sigma_d$) and aggregate interlock ($\tau_{agg}$) acting in normal and parallel to the crack plane, respectively. Values of the crack opening and sliding, in reference to the properties of the concrete and the aggregate, determine the contribution of these stress components. From the models presented for shear transfer mechanism, those represented by Walraven et al. [23], Bujadham [24] and Li [25] are most accurate. These models are defined on the basis of local displacement domain (opening and sliding) at the crack plane. However, finite element modeling is fundamentally defined upon strain-stress formulation. This eliminates the application of displacement-based shear models and inevitably results in introducing additional assumptions [9-11].

Application of the local-average stress field concept enhances the common finite element modeling by reliable estimation of the crack spacing. This is achieved by following the computational procedure of the proposed concept, especially step 5. Therefore, values of the crack opening and sliding are updated using Eq. 1-2, where the value of the crack spacing is calculated in reference to the local information and size-dependent parameters. This empowers the program of ESMARC with the application of the accurate displacement-based shear models. In this regard, the *contact density model*, presented by Li et al. [25] is implemented in the main body of the program. The strain values are transferred to the

displacement values with the aid of Eq. 1-2 and the complete formulation of the model is followed with no additional estimation.

Although the better estimation of the crack spacing is a distinct achievement of the local-average stress field concept, the exact modelling of size-dependent parameters in the shear response is more valuable. Size of the aggregate, size and material properties of reinforcing bars (especially yield state), tensile strength of concrete and the area of the crack plane are from the size-dependent parameters which are missed in simplified modelling of the shear response. Whereas, the local-average stress field concept enriches the modelling of this mechanism by automatic consideration of the size effects.

It is remarkable that in addition to the shear transfer mechanism, application of any local displacement-based models is also available by the proposed local-average stress field concept. This can be regarded as the most outstanding feature of the proposed approach which automatically detects the contribution of local mechanisms and size-dependent parameters.

## 4. DISCUSSION: CONTRIBUTION OF LOCAL MECHANISMS

The size-dependent behavior of lightly reinforced or unreinforced concrete members is more noticeable due to the formation of few cracks with large crack spacing. In such members, definition of the RC and PL zones with respect to the zoning concept must be followed by authentic judgments. However, this may bring inaccurate uncertainties into the average characteristics. Updating the local information during the analytical evaluation, the control volume is defined independent of any required judgment. To express the validation of the proposed concept, dependency of size in determining the tension softening behaviour of the plain concrete and tension stiffening of lightly reinforced concrete is discussed in this section.

As mentioned before, post-cracking tensile behaviour of a plain concrete is directly determined based on the release of the fracture energy. As it is discussed by Bazant in his Crack Band Theory [26], this release is fundamentally related to the crack width and depth. It means that for a constant width and depth, regardless of the element size, the amount of the released energy must be the same. However, definition of this release in the strain-based average models of smeared crack is followed by consideration of the size-dependent characteristics, especially localization of a crack in an element. For this aim, the pre-defined softening parameter of the cracked concrete is modified by the element size to have a total dissipated energy in the post-crack response equal to the $G_f$. This results in strain-stress models with different softening behaviour.

Adopting the local-average stress field concept, the average models are updated in accordance with the displacement domain. This approach satisfies the fundamental rules of the crack band theory with representing the similar tensile stress-crack width responses (Fig. 11a). In addition, updating the average models with respect to the local information, will reach to distinct models with different strain-stress responses, already introduced by smeared concept (Fig. 11b). It is remarkable that the mentioned outcomes of this approach are attained with automatic consideration of the size and the displacement domain.

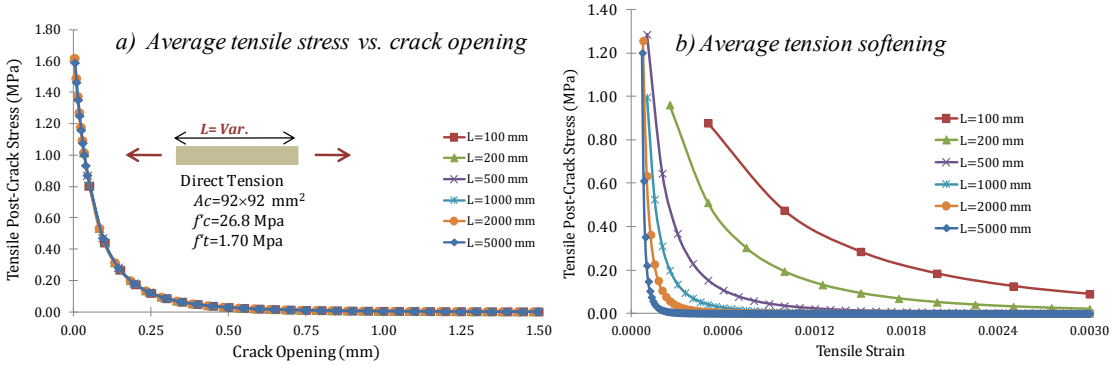


Figure 11. Dependency of size in reinforced and un-reinforced concrete

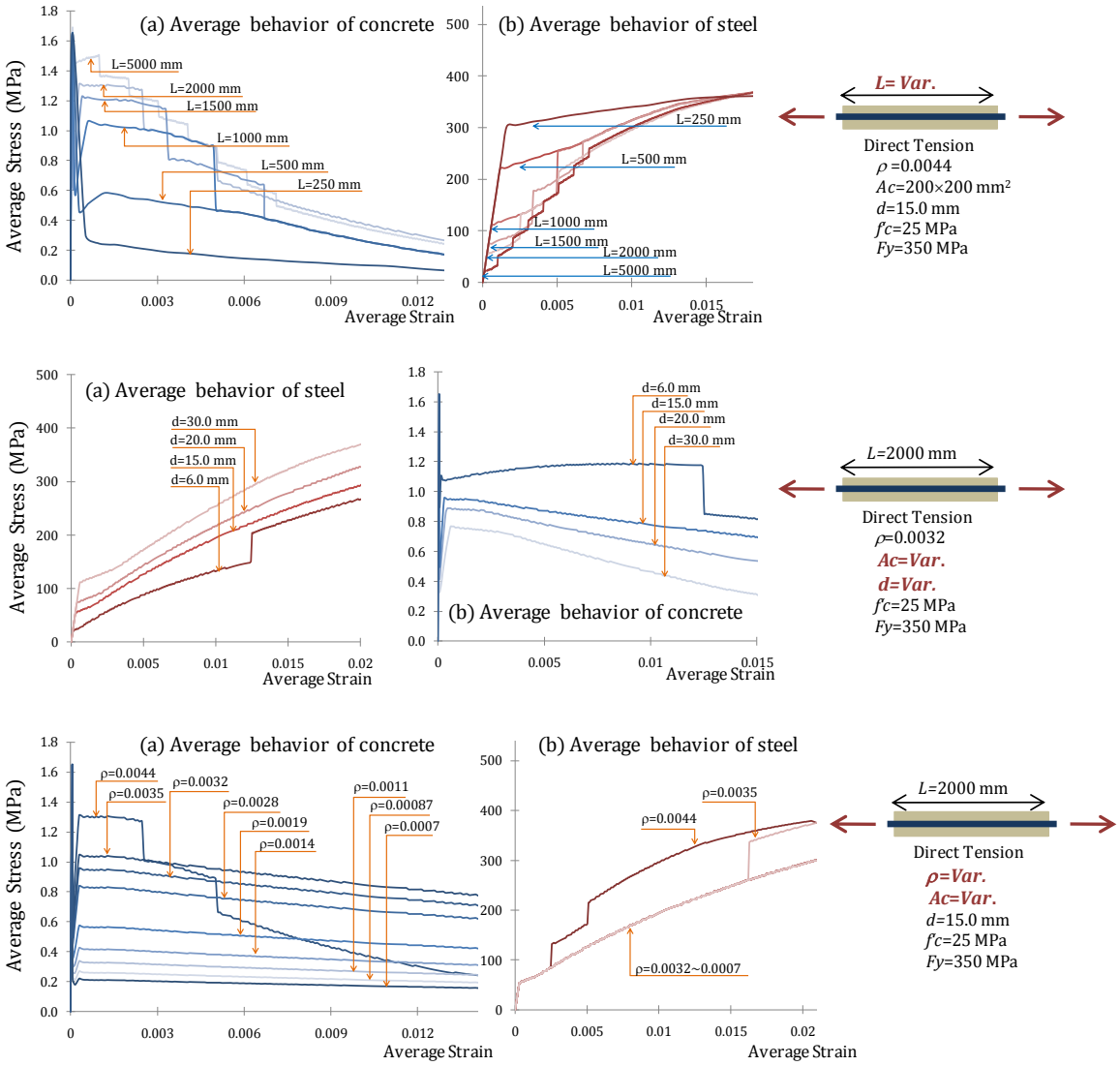


Figure 12. Parameter study on the effect of reinforcement diameter on the average behavior of materials

To express the effects of local mechanisms and size-dependent parameters in the average behavior of lightly reinforced members, three main studies have been conducted on the pure tension cases. Changing the values of crack spacing, reinforcement ratio and rebar diameter, average responses of concrete and steel bars are evaluated by the ESMARC program. According to the results presented in Fig. 12, the release in tensile stress of concrete in post-crack phase is almost different in comparison with the constant scheme considered by An [1]. The release is updated due to the local responses and the significant drops in this response are due to the new crack development. In addition, the behavior of steel is completely different with the average model adopted by smeared crack approach (Fig. 9). This is also followed by gradual increase in average yield stress and complies with occurrence of the cracks. Therefore, it is also different with the average yield stress determined as a constant value based on the zoning concept [9].

## 5. VERIFICATION

To investigate the accuracy of the proposed local-average stress field concept in evaluating shear-critical members, two main verifications are presented. In the first, RC panels under pure shear and combination of shear and axial stress [27] are evaluated. The panels are differently reinforced in longitudinal and transverse direction. However, the amount of embedded reinforcing bars is the same for both directions (Table 1).

Although the uniformity in pure shear case (PC1A) may lessen the participation of local mechanisms, the non-uniformity of the reinforcing ratio in two directions will cause the non-uniformity in the average response. In addition, presence of axial stress in PC4 and PC7 is followed by changing the crack angle. Therefore, contribution of concrete and both longitudinal and transverse reinforcing bars changes in comparison with the pure shear case.

Table 1: The specifications of RC panels [27]

| | Panel Series [A] | Concrete | | Horizontal Reinforcing [B] | | | | Vertical Reinforcing [B] | | | | Load case |
|---|---|---|---|---|---|---|---|---|---|---|---|---|
| | | $f'_c$ (MPa) | $\varepsilon_{peak}$ | Ratio (%) | D (mm) | $F_y$ (MPa) | Angle (Deg.) | Ratio (%) | D (mm) | $F_y$ (MPa) | Angle (Deg.) | $\tau_{xy}$: $\sigma_x$: $\sigma_y$ |
| PC | PC1A | 25.1 | 0.00183 | 1.65 | 5.72 | 500 | | 0.825 | 5.72 | 500 | | 1 : 0 : 0 |
| | PC4 | 24.9 | 0.00170 | 1.65 | 5.72 | 260 | 0.0 | 0.825 | 5.72 | 260 | +90 | 1:-0.39:-0.39 |
| | PC7 | 28.7 | 0.00185 | 1.65 | 5.72 | 390 | | 0.825 | 5.72 | 390 | | 1 : 0.32 : 0.32 |

[A] The dimensions of PC series is 890×890×70 mm.

[B] The elasticity module is defined as 196800, 202700 and 195000 MPa for PC1A, PC4 and PC7, respectively.

The overall shear strain-stress for the panels, with the individual behavior of the two reinforcing sets, is presented in Fig. 13. Regarding the results, 1) the estimated overall response shows agreeable consistency with the reported experimental result; 2) detected average behavior of reinforcing bars –whether horizontal or transverse- follows the reported

information of the tests; 3) average response of a reinforcing set in a distinct loading case is completely different with the two other loading cases. This shows the different effects of reinforcement arrangement in the three discussed panels.

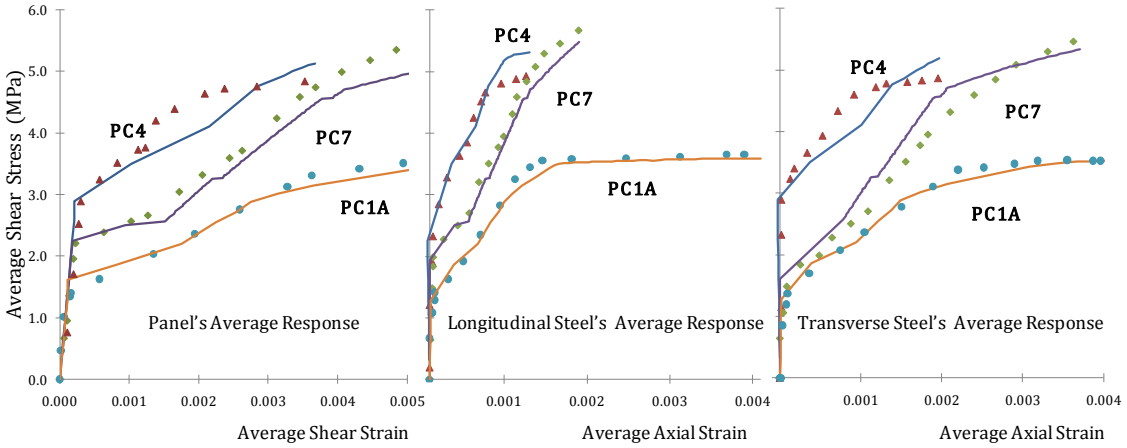


Figure 13. Total behavior of RC panels: Experimental and analytical results

In addition to the average characteristics derived by the aid of the proposed approach, crack spacing -as one of the effective size-dependent parameters in smeared crack modeling- is detected. Experimental and numerical values for the crack spacing are reported in Table 2. It shows that the reported value is agreeably consistent with the observed one.

Table 2: Reported Crack Spacing for PC panel series

| Panel \ Approach | PC1A | PC4 | PC7 |
|---|---|---|---|
| Experimental | - | 125~150 | 80~100 |
| Proposed Approach | 70.13 | 100 | 90 |

Table 3: The specifications of Scordelis shear beams [6]

| Beam | Concrete | | Longitudinal and Transverse Reinforcing [A] | | | Dimension (mm) | | | | |
|---|---|---|---|---|---|---|---|---|---|---|
| | $f'_c$ (MPa) | $f_t$ (MPa) | Bottom | Top | Shear reinf. | B | H | D | L | Span |
| OA-1 | 22.6 | 3.97 | 4 No. 9 | - | - | 310 | 556 | 461 | 4100 | 3660 |
| OA-2 | 23.7 | 4.34 | 5 No. 9 | - | - | 305 | 561 | 466 | 5010 | 4570 |
| OA-3 | 37.6 | 4.14 | 6 No. 9 | - | - | 307 | 556 | 462 | 6840 | 6400 |
| A-1 | 24.1 | 3.86 | 4 No. 9 | 2 No. 4 | No. 2 @ 210 | 307 | 561 | 466 | 4100 | 3660 |
| B-1 | 24.8 | 3.99 | 4 No. 9 | 2 No. 4 | No. 2 @ 190 | 231 | 556 | 461 | 4100 | 3660 |
| C-1 | 29.6 | 4.22 | 2 No. 9 | 2 No. 4 | No. 2 @ 210 | 155 | 559 | 464 | 4100 | 3660 |

[A] Yield strength of the steel bars: No.9: 555, No.4: 345, No.2: 325 MPa. Diameter of the steel bars: No.9: 28.7, No.4: 12.7, No.2: 6.4mm.

In the second verification set, shear-critical beams studied by Bresler and Scordelis [6] are evaluated by the proposed local-average stress field concept. As presented in Table 3, the beams are from different lengths, dimensions and reinforcing arrangements, with and without shear stirrups. Therefore, there are different participating mechanisms in each beam.

As an example, the beams with no stirrups will face with deep discrete cracks determining the ultimate shear strength of the beams. Pattern and characteristics of these cracks are affected by both dimension of the cross section and the length of the beam. The OA series, with quite similar cross sections, no shear reinforcement and different loading spans, are evaluated with quite reliable P-Δ response (Fig. 14). It can be interpreted that the proposed local-average stress field concept, and all corresponding details, has a great ability to detect the zones affected by the discrete cracks, even with different depth and forms. On the other side, the beam series of A-1, B-1 and C-1 have the same loading spans and are reinforced with the same amounts of stirrups. The effective parameters in determining the shear strength of these beams can be regarded by the width of the member and confinement properties of the stirrups. Due to the presented results (Fig. 14), it seems that following the control volume detection process and local stress field investigations has enriched the numerical analysis with an accurate estimation of each participating mechanisms. It is remarkable that differences in cross section dimensions and the span length of the beams are from the parameters activating the size-dependent responses of members. The results express the efficiency of the proposed concept in evaluating such size-dependent responses.

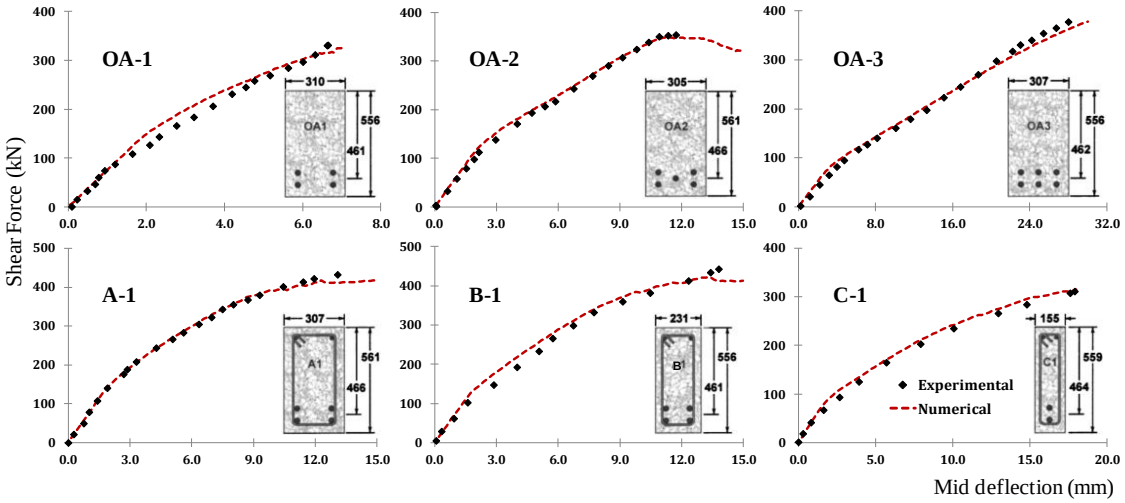


Figure 14. Scordelis Shear Beams: Experimental and analytical results

As it was mentioned before, the size effect in shear –by its common meaning- is regarded as the dependency of the shear strength to the depth of an RC member. This is investigated for the estimated shear strength of the beams studied by Stanik and Collins [8]. These beams were tested in different heights and lengths, with no shear reinforcement. Specifications of these beams are presented in Table 4. Reported values for the shear strength of the beams – experimental results and the values evaluated by code-based, existing numerical approaches, and the proposed concept- are presented in Table 5. Regarding the results, the concept can reliably estimate the shear strength of these beams as well. In addition, reduction in the shear

strength with respect to the increase in beam's depth is stated by the results presented in Fig. 15.

Table 4: The specifications of Stanik shear beams [8]

| Beam[A] | Longitudinal Reinforcing [B] | | Dimension (mm) | | | | |
|---|---|---|---|---|---|---|---|
| | Bottom | Web | B | H | D | L | Span |
| BN100 | 3 No.30 | - | 300 | 1000 | 925 | 6000 | 5400 |
| BN50 | 2 No.20<br>1 No.25 | - | 300 | 500 | 450 | 3000 | 2700 |
| BN25 | 3 No.15 | - | 300 | 250 | 225 | 1500 | 1350 |
| BN100D | 3 No.30 | 10 No.15 | 300 | 1000 | 925 | 6000 | 5400 |
| BN50D | 2 No.20<br>1 No.25 | 10 No.10 | 300 | 500 | 450 | 3000 | 2700 |
| BN25D | 3 No.15 | 10 No.3 | 300 | 250 | 225 | 1500 | 1350 |

[A] Compressive strength of concrete is reported by 37 MPa.
[B] Readers are recommended to follow the details of the reinforcement properties in reference [8].

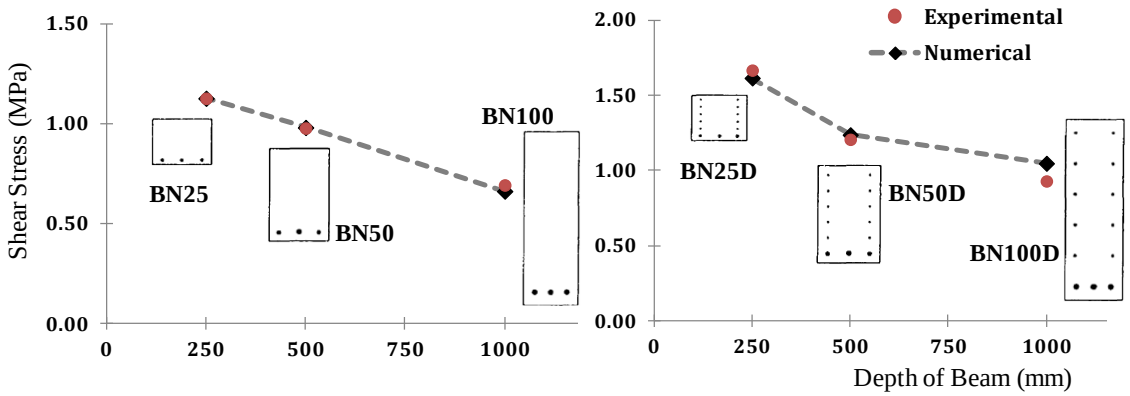


Figure 15. Stanik Shear Beams: Influence of member size on shear stress at failure

Table 5: Reported shear strength for Stanik beams [8]

| Beam \ Shear Strength | Experimental | Proposed Approach | ACI | MCFT [8] |
|---|---|---|---|---|
| BN100 | 192.1 | 183.6 | 281.9 | 189.2 |
| BN50 | 131.9 | 132.3 | 136.8 | 105.0 |
| BN25 | 73.0 | 76.0 | 68.4 | 61.0 |
| BN100D | 258.1 | 290.6 | 281.9 | 252.0 |
| BN50D | 162.9 | 167.0 | 136.8 | 141.5 |
| BN25D | 112.5 | 109.0 | 68.4 | 74.0 |

## 6. CONCLUSION

Numerical evaluation of RC members under shear would be improved with consideration of the size-dependent parameters and the post-crack mechanisms that affect the shear response. These features and their effects must be considered with respect to their dependency to the size. It is accurately regarded in the smeared crack approach by representing average constitutive models for reliable control volumes. Zoning concept as the most applicable theory for estimating the extent of the control volume enriches the smeared crack approach for consideration of the size-dependency in adequately reinforced members. However, formation of few cracks with large crack spacing in lightly reinforced members makes this concept to confront with uncertainties in the accurate evaluation of the control volume.

Following the fundamental average-based concept of the smeared crack, the *Local-average stress field* concept is proposed. The concept is enriched with proposed bond- and crack-influencing theories for automatic determination of the control volume considering the cracking progress. With the aid of a proposed slip-strain model, local distribution of strain/stress along the reinforcements embedded in the control volume is known. Accordingly, development of new cracks in the control volume and changes in the average properties of the constitutive models are detected. A better estimation of displacement at the crack plane is also attained; therefore, the displacement-based shear models would be applicable in the strain-based finite element formulation. In addition, the proposed concept is enriched with a computational process, regarding the local values for strain and displacement. This enables the concept for consideration of any size-dependent parameter or mechanisms. The abilities of the presented approach are discussed for unreinforced and reinforced concrete specimens and shear critical members. Regarding the results, the proposed concept firstly enhances the numerical procedure of the smeared crack approach with respect to the local information, and secondly, detects the effective size-dependent parameters by automatic step-by-step evaluation of the control volume. This is achieved by no significant increase in computational time and cost.

## REFERENCES

1. An X. *Failure analysis evaluation of seismic performance for reinforced concrete in shear*, PhD thesis, University of Tokyo, Japan, 1996.
2. An X, Maekawa K, Okamura H. Numerical Simulation of Size Effect in Shear Strength of RC Beams, *Proceedings of the Japan Society of Civil Engineers,* **564** (1997) pp. 297-316.
3. Kani GNJ. How safe are our large reinforced concrete beams, *Journal of the American Concrete Institute*, **64**(1967) 128-41.
4. Iguro M, Shioya T, Nojiri Y, Akiyama H. Experimental studies on shear strength of large reinforced concrete beams under uniformly distributed loads, *Concrete Library of the Japan Society of Civil Engineers*, **5**(1985) 137-54.

5. Shiyoa T, Okada T. The effect of the maximum aggregate size on shear strength of reinforced concrete beams, *JCI, 7th Annual Convention* (1985) 521-4.
6. Bresler B, Scordelis AC. Shear strength of reinforced concrete beams, *Journal of American Concrete Institute*, **60**(1963) 51-72.
7. Vecchio FJ, Shim W. Experimental and analytical re-examination of classic concrete beam tests, *Journal of Structural Engineering, ASCE*, **130**(2004) 460-9.
8. Podgornial-Stanik BA. The influence of concrete strength, distribution of longitudinal reinforcement, amount of transverse reinforced and member size, on shear strength of reinforced concrete members, PhD thesis, University of Toronto, Canada, 1998.
9. Maekaw K, Pimanmas A, Okamura H. *Nonlinear Mechanics of Reinforced Concrete*, Spon Press, England, 2005.
10. Vecchio FJ, Collins MP. The modified compression field theory for reinforced concrete elements subjected to shear, *Journal of the American Concrete Institute*, **83**(1986) 219-31.
11. Vecchio FJ. Disturbed stress field model for reinforced concrete: formulation, *ASCE Journal of Structural Engineering*, **126**(2000) 1070-7.
12. Belarbi A, Hsu TTC. Constitutive laws of concrete in tension and reinforcing bars stiffened by concrete, *ACI Structural Journal*, **94**(1994) 465-74.
13. Hsu TTC, Zhang LX. Tension stiffening in reinforced concrete membrane elements, *ACI Structural Journal*, **93**(1996) 108-15.
14. Rots JG, Blaauwendraad J. Crack models for concrete: discrete or smeared? fixed multi-directional or rotating?, *HERON*, **34**(1989) 1-59.
15. Broms BB. Technique for investigation of internal cracks in reinforced concrete members, *Journal of the American Concrete Institute*, Research report by the reinforced concrete research council, **62**(1965) 35-44.
16. Shima H, Chou L, Okamura H. Bond characteristics in post-yield range of deformed bars, *Proceedings of the Japan Society of Civil Engineers*, **10**(1987) pp. 113-124.
17. Soltani M, Maekawa K. Path-dependent mechanical model for deformed reinforcing bars at RC interface under coupled cyclic shear and pullout tension, *Engineering Structures*, **30**(2008) 1079-91.
18. Eligehausen R, Bertero V, Popov E. Local bond stress-slip relationships of deformed bars under generalized excitations, University of California, Berkeley, CA: Earthquake Engineering Research Center, Report No. 83-23, 1983.
19. FIP, Bond of reinforcement in concrete, State-of-art report, Fib bulletin No. 10, CEB-FIP, Lausanne, Switzerland, 2000.
20. Shima H, Chou L, Okamura H. Micro and macro models for bond in reinforced concrete, *Journal of the Faculty of Engineering, University of Tokyo (B)*, **39**(1987) 133-94.

21. Ghorbi E, Soltani M, Maekawa K. Development of a compressive constitutive model for FRP-confined concrete elements, *Composites: Part B*, **45**(2013) 504-17.
22. Salem HMM. Enhanced Tension Stiffening Model and Application to Nonlinear Dynamic Analysis of Reinforced Concrete, PhD Thesis, Tokyo University, 1998.
23. Reinhardt HW, Walraven JC. *Aggregate Interlock and Dowel Action under Monotonic and Cyclic Loading*, Delft University Press, 1988.
24. Bujadham B, Maekawa K. The universal model for stress transfer across cracks in concrete, *Proceedings of the Japan Society of Civil Engineers*, **451**(1992) pp. 277-87.
25. Li B, Maekawa K, Okamura H. Contact density model for stress transfer across cracks in concrete, *Journal of the Faculty of Engineering, the University of Tokyo (B)*, **XL**(1989) 9-52.
26. Bazant ZP, Oh BH. Crack band theory for fracture of concrete, *Materials and Construction*, **16**(1983) 155-77.
27. Vecchio FJ, Chan CCL. Reinforced concrete membrane elements with perforations, *Canadian Journal of Civil Engineering*, **17**(1990) 698-704.